USE OF DIGITAL IMAGE CORRELATION ANALYSIS FOR DAMAGE STATES IDENTIFICATION IN CONCRETE BLOCK MASONRY WALLS

Bennett Banting[1] and Wael El-Dakhakhni[2]

[1] Ph.D., Department of Civil Engineering, McMaster University, Hamilton, ON, Canada, bantinbr@mcmaster.ca
[2] Martini, Mascarin and George Chair in Masonry Design, Co-Director, Centre for Effective Design of Structures, Department of Civil Engineering, Hamilton, ON, L8S 4L7, Canada, eldak@mcmaster.ca

ABSTRACT

The use of digital image correlation (DIC) has been prevalent in aeronautical and mechanical engineering fields for several decades. It is only recently that with the commercial availability of high resolution digital cameras and analysis software that it has become common within large scale testing of concrete and masonry structural elements. Three walls were instrumented and tested using digital image correlation to measure strains on the wall surface. In this paper, the measurements taken represent a simplified and accurate means of measuring surface crack widths as well as deformation in the walls. An equation is proposed to estimate flexural crack widths from traditional LVDT measurements for curvature and these values are compared to those collected from DIC. Based on this analysis combined with more traditional observations, the definition and identification of damage states within boundary element walls was defined towards the development of the next-generation of seismic design codes. Based on this technique, each damage state can be linked with the type of method of repair as well as the extent of such a repair method.

KEYWORDS: concrete block, design codes, shear wall, shear strength

INTRODUCTION

As part of the planned changes to the next edition of the masonry structures design standard in Canada, the CSA S304, a new category of seismic force resisting system (SFRS) has been proposed. Although not currently applicable within Canadian seismic design, the development of next-generation seismic design methodologies also requires experimental data and analysis of these new reinforced masonry (RM) shear wall categories within the context of next-generation displacement- and performance-based seismic design methodologies. In the U.S.A. this task is currently being undertaken by the Applied Technology Council (ATC) which is under contract by the Federal Emergency Management Agency (FEMA). FEMA document P695 [1] sets out the required information for different building systems including the testing of isolated structural components in the manner prescribed by FEMA 461 [2]. The information generated will ultimately be used for the development of backbone curves and fragility functions according to the methodology set out by ATC-58 [3] to be used by stakeholders and designers of structures.

In Canada, the Standing Committee on Earthquake Design (SC-ED), acting within the mandate of the National Building Code of Canada, will be looking into adoption of seismic performance-based design methods [4] as of the 2020 edition. In this regard, performance-based seismic

design parameters related to the occurrence of damage-based indicators require quantification. The latest guide referring to the identification of damage states was published in the FEMA 306 document [5]. Damage states were defined by their associated method of repair (MOR), indicative of the cost associated with structural rehabilitation after a seismic event. As part of a larger study, three shear walls with boundary elements were tested and monitored using digital image correlation (DIC) analysis software as a means to measure key performance-based indicators such as crack width, which will be presented in this paper.

The use of DIC has long been associated with measuring the deformation and fracture of metallic materials, but has found more recent applications towards concrete and masonry materials testing. Choi and Shah [6] tested prismatic concrete specimens under compression and indicated a good correlation between DIC and typical displacement transducer (LVDT) measurement techniques towards measuring compressive strain. In their study, DIC was also used to measure surface strains on the concrete specimens including quantifying the formation of cracks within the cement matrix. Lawler and Keane [7] measured deformations in concrete subject to compression using 3-D DIC analysis. Similarly, Raffard et al. [8] applied DIC towards the testing of historical stone masonry materials, however, as with the previous authors' work, specimens were of a relatively small size compared to structural elements. More recently, Tung et al. [9] applied DIC towards compression test of brick panels and both Tusini and Willam [10] and Citto et al. [11] reported using DIC analysis in tests on brick prism compression tests. Much of the research related to masonry materials which has documented use of DIC has focused on small scale compression testing, although Smith et al. [12] reported using DIC towards the analysis of full-scale testing of precast concrete shear walls subjected to lateral loads. While, Destrebecq et al. [13] used DIC towards crack detection of reinforced concrete beams. DIC has demonstrated to be an accurate technique of measuring surface deformations at the small scale, but with improvements in technology and ready availability of high resolution of digital cameras, has been expended to full-size structural elements. The purpose of this test program is to apply DIC measurement techniques towards quantifying surface wall deformations, flexural curvatures and crack propagation in masonry shear walls.

EXPERIMENTAL PROGRAM

Three walls were constructed with boundary elements as part of a larger experimental study. The experimental test set-up and observations have been presented elsewhere in greater detail [14], however a summary of the test wall is described in this section for completeness. A half-scale version of the standard 190 mm x 190 mm x 390 mm concrete block stretcher unit (typical to North American construction) was specified for construction of the walls. The 90 mm x 90 mm x 185 mm half-scale blocks were laid with a 5 mm scaled mortar joint in a half running bond by professional masons. The walls each possessed confined boundary elements which were comprised of two units laid together resulting in an overall boundary element cross sectional size of 185 mm x 185 mm and reinforcement with lateral stirrups for buckling prevention. The three walls were each constructed with a length (ℓ_w) of 1,235 mm, with Wall 1 constructed to a height (h_w) of 1,900 mm and Walls 2 and 3 constructed to a height of 2,660 mm and different reinforcement ratios as indicated in Table 1 and Fig.1.

Table 1: Summary of the Boundary Element Shear Walls Tested incorporating DIC

Wall	Length (ℓ_w)	Height (h_w)	Vertical Reinforcement Ratio (ρ)
1	1,235 mm	1,900 mm	0.69%
2	1,235 mm	2,660 mm	0.69%
3	1,235 mm	2,660 mm	1.17%

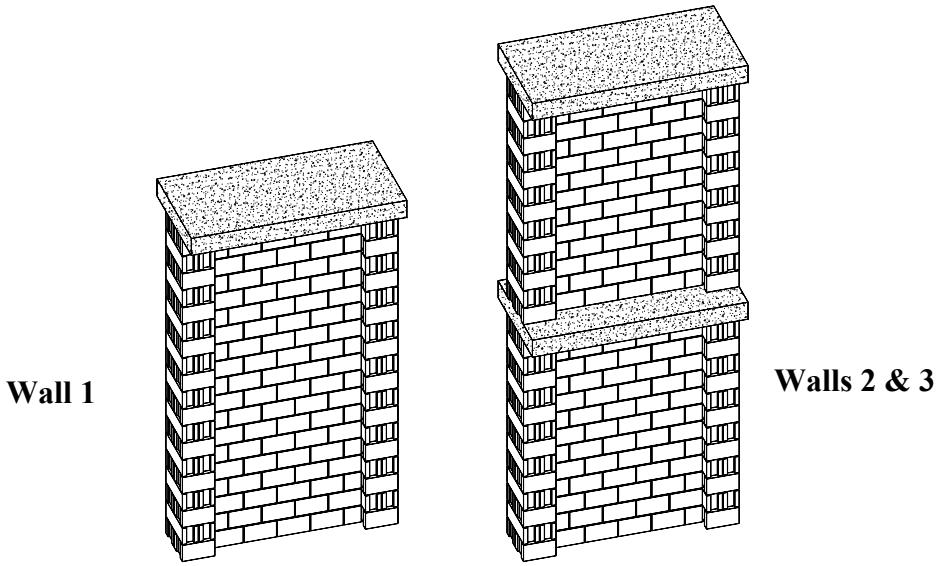

Figure 1: Isometric View of Walls Possessing Confined Boundary Elements Tested

Testing was conducted for each wall through load-control protocol with initial lateral loads applied along the tops of the walls at increments of 25% of the theoretical yield load. The top displacement of the wall measured at this point was averaged from both directions of loading and is defined as the experimental yield displacement. Further displacement-controlled loading cycles of the wall were then applied at increasing multiples of the yield displacement representing values of the experimental displacement ductility. A full displacement cycle consists of the displacement measured at the top of a wall from a zero load starting position to the target displacement in the West direction (+) then reversed to the same displacement in the East direction (–) and subsequently brought back to the point of zero load.

DIC INSTRUMENTATION AND CALIBRATION

Preparation of the walls for analysis required a black and white random speckle pattern to be pained on one side of the walls as shown in Fig. 2. A 14 mega-pixel camera was fixed in place and used to take black and white digital photographs of the wall during testing at each displacement cycle. The size of the walls, speckle pattern and resolution of the cameras resulted in an effective image size of 1 pixel equivalent to an average area of 0.25 mm^2. For a successful analysis, black speckles should be between 10 – 30 pixels in size [15], which is required for the default settings in the software. The software will analyze the pattern within a grid size of 27 pixels × 27 pixels. Pictures of each wall were taken just prior to testing to act as the reference image, with subsequent photos taken at the peak displacement of each displacement cycle. The

DIC algorithms then trace the relative movement of pixels over the load history of a test specimen as it deforms. This is accomplished by first assigning a grid of nodes to the area of interest defined on the reference image, as depicted in Fig. 3. Analysis begins with a pixel pattern, acting as a point of reference on the walls, which subsequent images are compared to. Analysis of the nodes within the reference grid is then compared to the adjacent grid of pixels, which is defined based on the step size chosen, the default is 5 pixels over from the first. From this, the software maps the location and intensity of the pixels in the reference image and compares them to the deformed image as indicated in Fig. 3. The use of the default settings results in a confidence level of deformation measurements of 0.1 pixels (0.05 mm). Acceptability of a DIC analysis is verified by the number of calculation iterations required, whereby analysis of the walls with the default settings resulted in an average of 1.9 to 2.3 iterations, a number less than five indicates an accurate measurement [15].

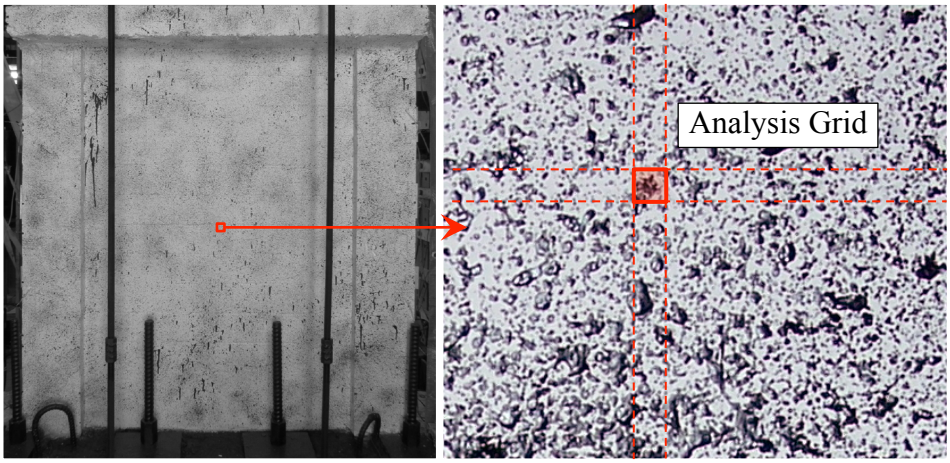

Figure 2: Random Black and White Painted Speckle Pattern

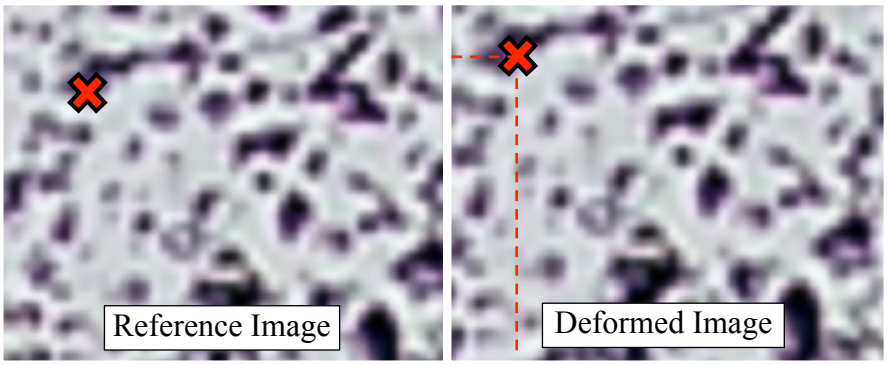

Figure 3: Tracing the Movement of Pixels from the Reference Image

Since the walls were also measured using conventional LVDTs mounted on the walls during testing, calibration and comparison of the DIC measurements to the LVDTs was conducted. During early load cycles of the walls it became evident that as a result of the resolution of the paint speckle pattern as well as digital cameras used to record pictures of the walls, it was not possible to gather reliable measurements of very low elastic strains on the surface of the wall.

However, because these walls were considered to be highly ductile, and the main objectives of the DIC analysis was in damage analysis, measurements at such very low load levels that masonry remains uncracked were not of interest within this study. DIC analysis returns relative surface strains and displacements of the walls' surface in terms of relative pixel size. To facilitate comparison with LVDT measurements, the reference image for each wall, taken prior to loading, is used to calibrate between pixel size and physical dimension. To reduce lens effects and due to limitations with digital cameras and laboratory space, Walls 2 and 3, were recorded by two separate cameras, with one trained only on the lower storey of the wall (1.3 m tall) and the second trained on the upper storey. This was selected since the concentration of plastic hinging and cracking damage was anticipated to be contained within the lower storey only. The DIC images were then calibrated based on physical markers of a known physical dimension on the walls and the area of the wall is selected for analysis (omitting components of the test set-up that are in the field of view) as indicated in Fig. 4a, which on average resulted in a calibrated pixel size of 0.5 mm × 0.5 mm. The deformations interpreted from DIC could be plotted as either vertical displacement (indicative of flexural curvature) in Fig. 4b or as horizontal displacement (indicative of lateral deformations) in Fig. 4c.

The exact locations of the LVDTs were subsequently mapped on the DIC reference image for each test wall as shown in Fig. 5a and the vertical displacements were exported over the load histories for each wall. Comparison between physical LVDT and DIC measurements for wall displacement revealed that at high levels of displacement, the upper floors of Wall 2 began to show deviation from LVDT measurements. This was later attributed to play within the out-of-plane support system in the test set-up which caused slight movements in the wall, normal to the wall's lateral movements being recorded. Nevertheless, such erroneous readings were limited to the top of the aforementioned wall only, and were absent from Walls 1 and 3. Overall, DIC and LVDT measurements were within ± 0.5 mm to each other on average, within operating parameters of the LVDTs. The use of DIC at very high displacement cycles was hindered by the occurrence of face shell spalling and separation. It was observed that DIC became ineffective in areas where the heaviest damage occurred, a similar issue with surface-mounted LVDTs.

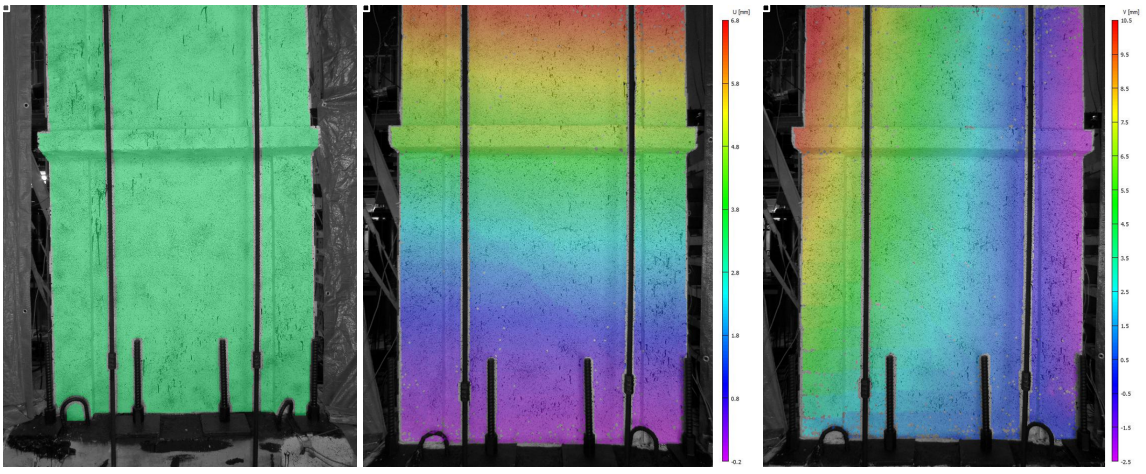

a) **b)** **c)**

Figure 4: Results of DIC Analysis: a) Area of Interest Defined as the Surface of the Wall, b) Indicating Lateral Displacements in the Wall, and c) Indicating Vertical Displacements in the Walls

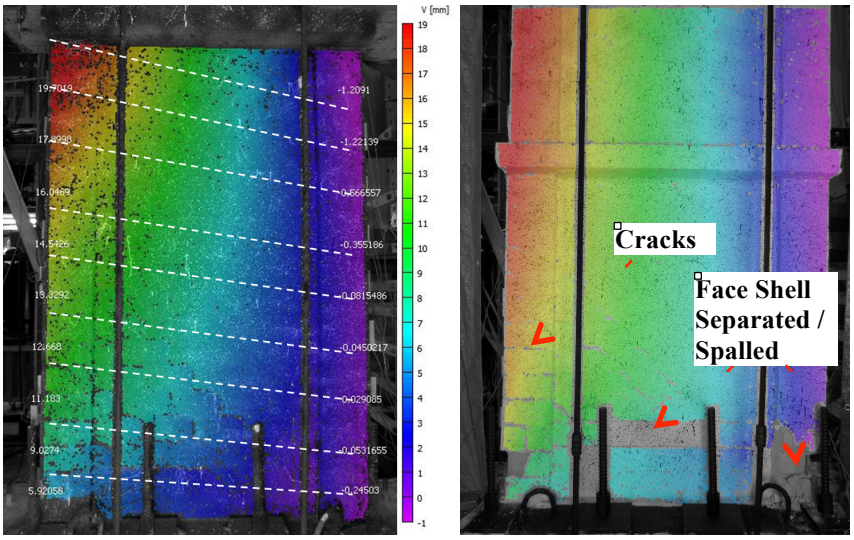

a) **b)**

Figure 5: DIC Measurements of Walls: a) Vertical displacement readings as LVDT Locations Indicating Flexural Curvature in the Walls (Dashed Lines), and b) Loss of DIC Measurements at Very High Drifts (>2.5%) when Crushing and Spalling has Occurred

CRACK MEASUREMENTS

The DIC analysis produced average strains on the surface of each wall over its load history, whereby, crack widths could be mapped directly by the software at areas where tensile flexural and shear strains were concentrated. This process is expedited within masonry because of the tendency for tensile strains to be concentrated in the inherent planes of weakness formed by the mortar joints. It was made evident during testing that crack damage was predominantly characterized by horizontal cracks along the bed joints due to flexural bending. The graphical analysis produced by DIC of vertical strains illustrates this observation, as indicated in Fig. 6, which depicts the first observed formation of flexural cracking at a top drift of ± 0.15% and load equal to 75% the yield load in Fig. 6a and 6b for Wall 2. This can be compared with the increase in crack penetration at a top drift of ± 1.2% and at peak lateral resistance in Fig. 6c and 6d. Vertical strain concentrations, illustrated as yellow and red, are localized at each bed joint in the boundary elements, even when not visually observed during testing. The peak tensile strains in Fig. 6a and 6b were recorded as 0.8%, increasing to 3.0% in Figures 6c and 6d. It is evident from the previous figure that as cracks develop portions of the mortar or faceshell will spall away and the DIC analysis will no longer be able to measure strains, indicated by small grey patches in Fig. 6c and 6d.

To account for this, cracks are measured by the relative displacement of adjacent segments above and below a crack as illustrated in Fig. 7 using the software's crack measuring tool. Based on the image correlation analysis as well as observations made during testing, the maximum crack widths over the load history for Walls 1, 2 and 3 were contained within the boundary element and web of wall adjacent to the boundary element in the lower courses of the walls. These cracks were predominantly associated with flexure, however, shear crack widths were also measured, and were found to be the largest, although still smaller than flexural crack widths, in the web of the walls somewhere between the middle of the wall and the tension boundary element. The median crack width (δ_c) of the largest crack was selected as the parameter of interest for each

walls' load cycle to be incorporated with damage state definition. The median, rather than mean, was chosen due to the potential for abrupt changes in the crack width due to the irregular cack surface. These peaks of troughs in crack width, illustrated in Fig. 7b, tended to skew mean crack measurements.

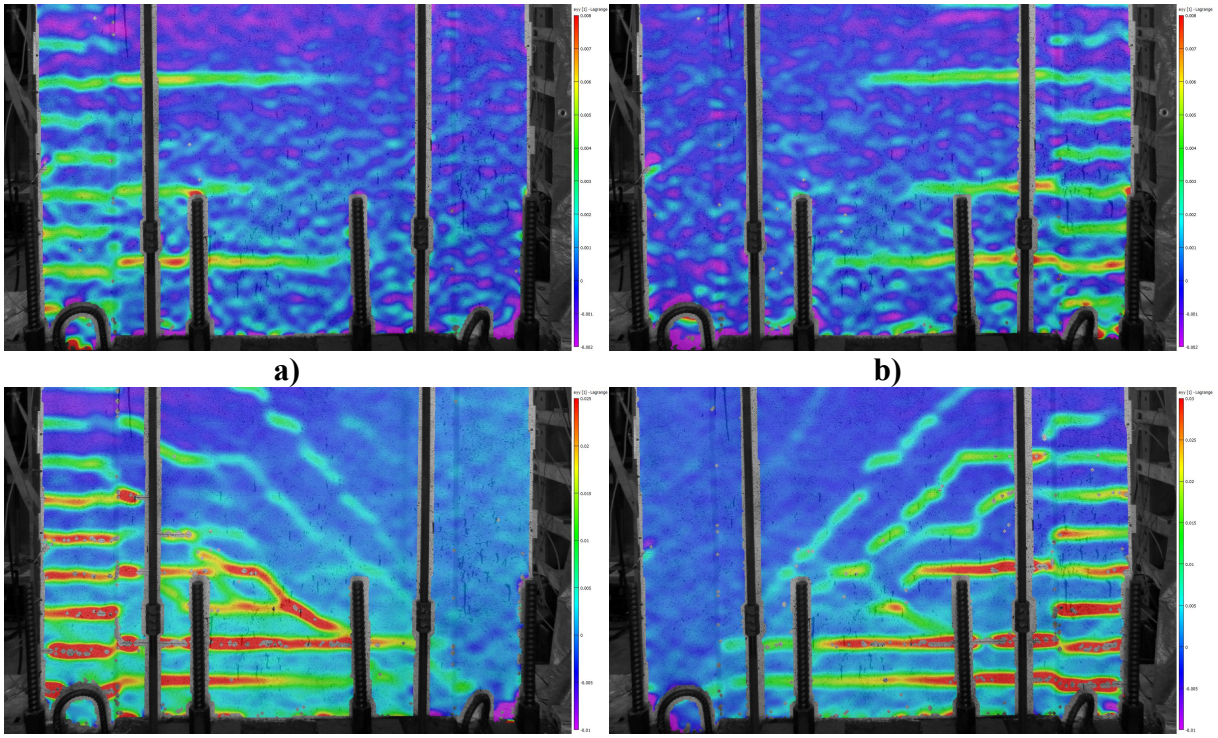

a) b) c) d)

Figure 6: Vertical Strain Concentration in Bed Joints of Wall 2: a) 75% Yield Load in +ve Load Direction, b) 75% Yield Load in -ve Load Direction, c) Peak Lateral Resistance in +ve Load Direction and d) Peak Lateral Resistance in –ve Load Direction

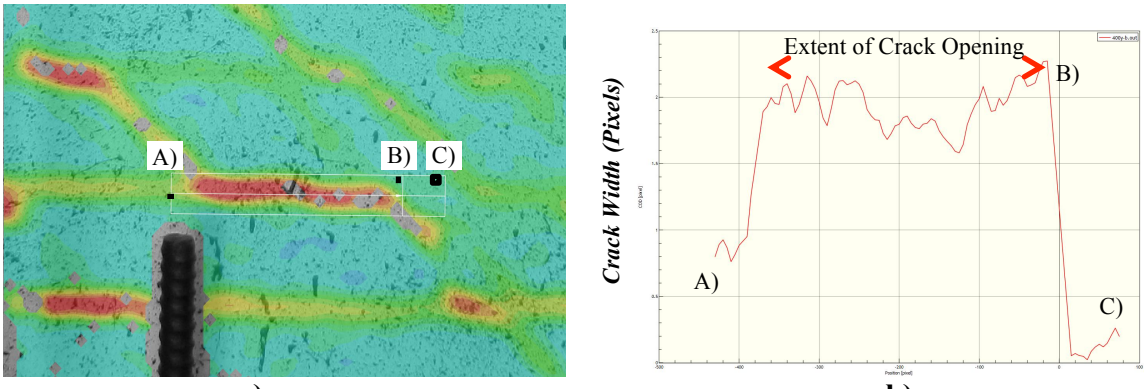

a) b)

Figure 7: Determining Crack Widths in Walls: a) Close Up of a Crack Formation with Crack Measuring Tool, and b) Plot of Measured Relative Deformation over Crack Length Indicating Crack Width

The measured crack widths for the walls are depicted in Fig. 8 after being converted into mm over the load histories of the walls and from both directions of loading. Overall, peak flexural

crack width demonstrated a nearly linear relationship with drift for all walls, indicated by the best fit lines and the values of R^2 close to 1.0:

- Wall 1: δ_c = (140 × Top Drift) - 0.17 (R^2 = 0.97)
- Wall 2: δ_c = (135 × Top Drift) - 0.05 (R^2 = 0.98)
- Wall 3: δ_c = (116.5 × Top Drift) - 0.16 (R^2 = 0.98)

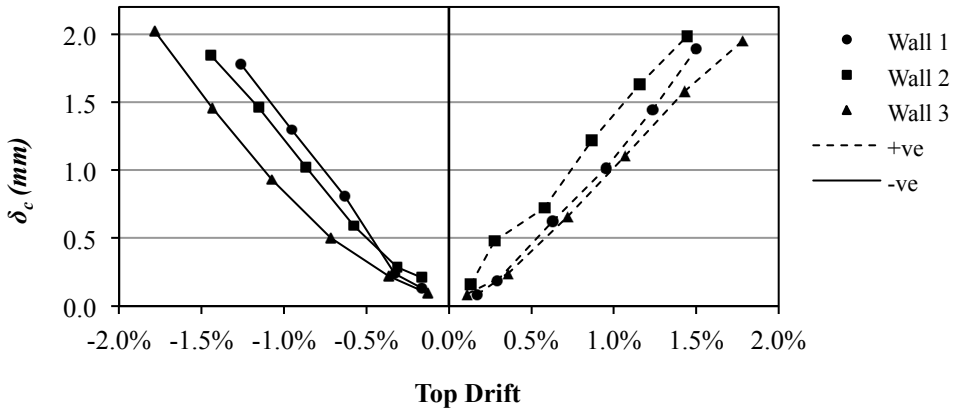

Figure 8: Crack Widths of Walls over Loading History

Therefore, based on the observations of Fig. 8, it is theorized that it may be possible to establish a theoretical basis to measure crack widths based on curvature readings in the walls and taking advantage of the knowledge that crack locations being are exclusively concentrated at the mortar joints as indicated from the DIC curvature measurements depicted in Fig. 9a.

The crack width determined from the average curvature measurements is evaluated from the LVDT measurements which recorded the vertical strains over the bottom four courses of the walls (4 mortar joints in total) and is defined as δ_ϕ. Two conservative assumptions are made to estimate δ_ϕ: no tensile strains are carried in the masonry between cracks which are concentrated at the bed joints (neglecting tension stiffening) and crack widths are evenly distributed between the bottom four mortar joints. Therefore, δ_ϕ is determined from the curvature measurement at the base of the wall (ϕ), the depth of neutral axis (c) and a crack spacing of 95 mm (s_c), based on the half-scale nominal unit height, from Eq. 1.

$$\delta_\phi = \phi(\ell_w - c)s_c \tag{1}$$

The ratio between observed cracks from the image correlation analysis and those calculated from curvature measurements (δ_c / δ_ϕ) for Walls 1, 2 and 3 is plotted in Fig. 9b. Overall, an average ratio between curvature and digital image correlation crack width measurements of δ_c / δ_ϕ = 0.88 (c.o.v. = 14.9%) was determined, indicating a fairly good correlation between the two methods.

To relate this data to full-scale masonry construction, for which the FEMA 306 crack limits have been established for, the data given in Fig. 9b will have to be scaled to consider the increased spacing. It is expected that curvatures will not differ from half-scale to full-scale walls, since

material strain limits are assumed to be constant and the depth of neutral axis remains as a constant proportion of wall length [16]. However, the space between flexural cracks (s_c) would be increased to reflect the increased height of units, set to a nominal height of 200 mm. Applying these modifications to Eq. 1 for the walls provides a representative estimate of the equivalent full-scale crack width. From the perspective of performance-based design, only the minimum top drift from either direction of loading that is associated with the first occurrence of one of the predefined crack limits given in FEMA 306 would be of interest.

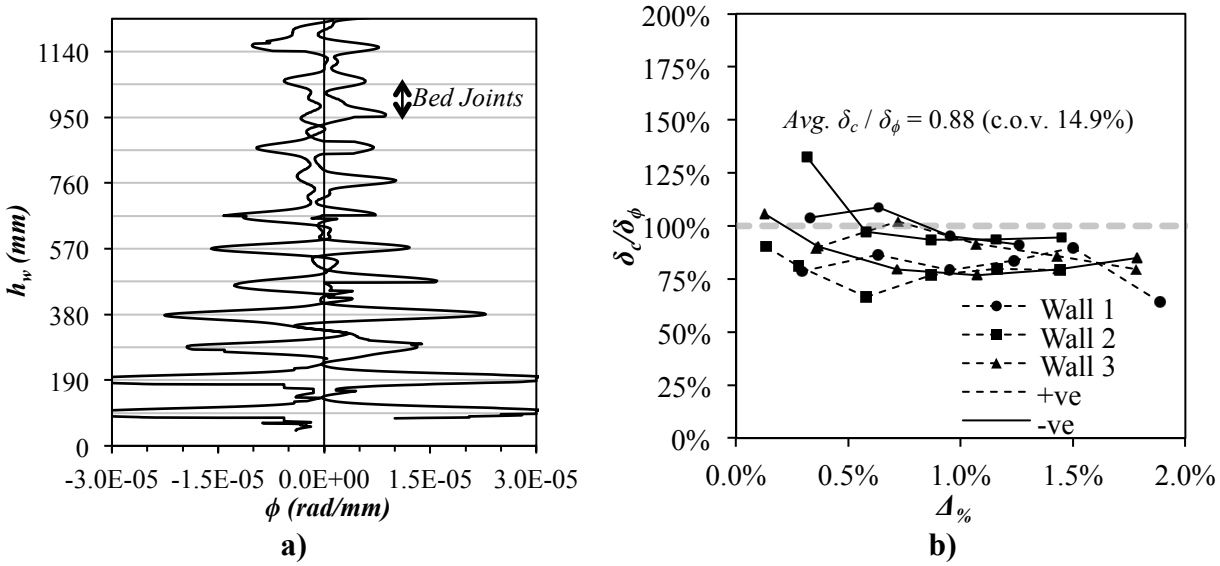

Figure 9: DIC Cracks: a) DIC Curvature Concentrated at Bed Joints, and b) Comparison between LVDT and DIC Flexural Cracks

CONCLUSIONS

Digital image correlation (DIC) analysis has been applied towards the measurements of flexural surface strains and deformations of three shear walls tested under reversed cycles of quasi-static lateral displacement. A common drawback of DIC analysis of larger masonry elements, such as shear walls, is that it is difficult to accurately measure elastic strains, a problem also shared with more traditional LVDT instrumentation. However, it was established that DIC proved to work as an accurate means to measure strains and displacements in the wall when large inelastic tensile strains were present. It was also confirmed through DIC analysis that even in the fully-grouted walls, flexural crack formation and propagation was localized within the bed joints, which act as predefined planes of weakness. Overall a strong correlation was found between wall displacement and maximum flexural crack width that would facilitate establishing the required method of repair within performance-based seismic design. Because of the observation of the most critical flexural crack damage is localized along the bed joints, an equation was proposed to relate curvature measurements from LVDTs to the peak crack width.

ACKNOWLEDGEMENTS

Financial support has been provided by the McMaster University Centre for Effective Design of Structures (CEDS) funded through the Ontario Research and Development Challenge Fund (ORDCF) as well as the Natural Sciences and Engineering Research Council (NSERC) of Canada. Provision of mason time by Ontario Masonry Contractors Association (OMCA) and

Canada Masonry Design Centre is appreciated. The supply of half-scale blocks by the Canadian Concrete Masonry Producers Association (CCMPA) is gratefully acknowledged.

REFERENCES

1. Applied Technology Council. (ATC). (2009). "Quantification of building seismic performance factors." Federal Emergency Management Agency (FEMA) P695, Washington D.C., USA.
2. Applied Technology Council. (ATC). (2007). "Interim testing protocols for determining the seismic performance characteristics of structural and non-structural components." Federal Emergency Management Agency (FEMA) 461, Washington D.C., USA.
3. Applied Technology Council (ATC). (2011). "Seismic performance assessment of buildings Volume 1 - methodology." ATC-58-1 75% Draft, ATC, Redwood City, CA.
4. Standing Committee on Earthquake Design (SC-ED). (2010). "Canadian Commission on Building and Fire Codes Meeting Agenda Item Summary Sheet." Report on Activities and Work Plan, National Research Council Canada, Ottawa, Canada, <http://www.nationalcodes.ca/ccbfc/letterballot/346/23.14.9a%20ED%20Report%20and%20request.pdf> (Accessed Jan., 2011)
5. Applied Technology Council. (ATC). (1998). "Evaluation of earthquake damaged concrete and masonry wall buildings." FEMA 306, Washington D.C., USA.
6. Choi S., Shah, S.P. (1997). "Measurement of deformation on concrete subject to compression using image correlation." Experimental Mechanics, 37(3), 307–313.
7. Lawler, J., and Keane, D. (2001). "Measuring three-dimensional damage in concrete under compression." ACI Materials Journal, 98(6), 465-475.
8. Raffard D., Ienny P., and Henry, J. P. (2001) "Displacement and strain fields at a stone/mortar interface by digital image processing." J. Testing & Eval., 29(2), 115–122.
9. Tung, S., Shih, M., and Sung, W. (2008). "Development of digital image correlation method to analyse crack variations of masonry wall." Sadhana, 33(6), 767-779.
10. Tusini, E., and Willam, K. (2008). "Performance evaluation of reinforced concrete masonry infill walls." Report CU-NEES-08-04, Centre for Fast Hybrid Testing, University of Colorado, USA.
11. Citto, C., Wo, S. and Willam, K. (2011). "Image correlation diagnostics of masonry assemblies." Proc., 11th North American Masonry Conference, Minneapolis, Minnesota, Paper #6.02-1.
12. Smith, B. J., McGinnis, M. J., and Kurama, Y. C. (2010). "Full-field lateral response investigation of hybrid precast concrete shear walls." 3rd fib International Congress, Washington D.C., USA.
13. Destrebecq, J. F., Toussaint, E., and Ferrier, E. (2010). "Analysis of Cracks and Deformations in a Full Scale Reinforced Concrete Beam Using a Digital Image Correlation Technique." Experimental Mechanics. 51(6), 879-890.
14. Banting, B. R. and El-Dakhakhni, W. W. (2012). "Seismic performance quantification of reinforced masonry structural walls with boundary elements." Submitted to J. Struct. Eng.
15. Cintrón, R. and Saouma, V. (2008). "Strain measurements with digital image correlation system Vic-2D." Report Cu-NEES-08-06, University of Colorado, U.S.A.
16. Harris, H. G. and Sabnis G. M. (1999). Structural Modelling and Experimental Techniques. 2nd ed., CRC Press, New York, U.S.A.